CSMA 2019
14ème Colloque National en Calcul des Structures
13-17 Mai 2019, Presqu'île de Giens (Var)

Granulation of wet granular media in rotating drum

T.T. Vo[1,2], S. Nezamabadi[1,3], P. Mutabaruka[1], J.-Y. Delenne[3], F. Radjai[1]

[1] *LMGC, CNRS, Université de Montpellier, {thanh-trung.vo, franck.radjai, saeid.nezamabadi, patrick.mutabaruka}@umontpellier.fr*
[2] *Bridge and Road Department, Danang Architecture University, 553000 Da Nang, Vietnam*
[3] *IATE, CIRAD, INRA, Montpellier SupAgro, Université de Montpellier, jean-yves.delenne@inra.fr*

Résumé — We study the agglomeration process of wet granular materials in a rotating drum by using discrete-element simulations. The particle interactions account for the cohesive and viscous forces of the binding liquid. We assume that the liquid is transported by wet particles and keeps a constant volume during granulation. A single granule introduced into the rotating drum grows by capturing wet particles. We find that the granule size increases exponentially with the number of drum rotations, and we investigate the effects of various parameters on the growth process.
Mots clés — Granular matter ; Granulation ; Capillary bond ; Discrete Element Method ; Rotating drum.

1 Introduction

The agglomeration of solid particles is a fundamental process in industrial applications such as the manufacture of pharmaceuticals, fertilisers, powder metallurgy and iron-making. Wet agglomeration occurs as a result of the collisions of moist particles in a flowing granular bed. The particle size increase modifies the density and strength of a granular material, and it may improve its flow properties, reduce the segregation of different types of particles, and increase the permeability [1]. The particles are wetted by mixing raw particles with the binding liquid [2]. The nuclei of granules are formed due to the collisional and frictional or capillary and viscous interactions between wet primary particles and by the incorporation of the binding liquid [3].

The size, strength, and texture of granules depend on the process and material parameters. The process parameters include the amount of liquid volume, the size ratio between the drum and mean particle diameter, the rotation speed, the inclination angle, and the filling rate [8, 7, 6]. The material parameters are the binding liquid and raw material properties including the liquid viscosity, particle size distribution, mean particle size and friction coefficient of particles [2]. The agglomeration of wet particles involves three elementary processes : wetting and nucleation, accretion and growth, and erosion (or attrition) and breakage [9]. A granule grows if the accretion rate is larger than the erosion rate. The growth will eventually stop if the liquid volume is finite (no liquid supplied). In continuous supply of liquid, the granule growth can continue until all particles are wetted and as long as the liquid is in the funicular state (no slurry).

In this paper, we use the Discrete Element Method (DEM) to simulate the evolution of a single small granule initially introduced into a rotating drum. The primary particles in the drum are either wet or dry. The wet particles interact through a capillary-viscous force law, and their number represents the amount of liquid inside the drum. We analyze the effects of various material parameters on the evolution of the granule.

2 Numerical method and granulation procedure

2.1 Numerical method

We use a Molecular Dynamics (MD) approach for DEM simulations of the agglomeration process. The motion of each solid spherical particle i of radius R_i is governed by Newton's second law. The particles interact through five different forces : the normal contact force f_n, the tangential friction force

f_t, the capillary attraction force f_c and the viscous force f_{vis} [12] :

$$\begin{aligned} m_i \frac{d^2\mathbf{r}_i}{dt^2} &= \sum_j [(f_n^{ij} + f_c^{ij} + f_{vis}^{ij})\mathbf{n^{ij}} + f_t^{ij}\mathbf{t}^{ij}] + m_i\mathbf{g} \\ \mathbf{I}_i \frac{d\boldsymbol{\omega}_i}{dt} &= \sum_j f_t^{ij}\mathbf{c}^{ij} \times \mathbf{t}^{ij} \end{aligned} \tag{1}$$

where m_i, $\mathbf{I}_i$, $\mathbf{r}_i$, $\boldsymbol{\omega}_i$ and $\mathbf{g}$ denote the the mass, the inertia matrix, and the position, rotation and gravity acceleration vectors of particle i, respectively. $\mathbf{n}^{ij}$ is the normal vector of the contact plane between the particles i and j, $\mathbf{t}^{ij}$ denotes the tangential vector belonging to the contact plane ij and pointing in the direction opposite to the relative displacement of the two particles and $\mathbf{c}^{ij}$ is the vector pointing from the center of particle i to the contact point with particle j.

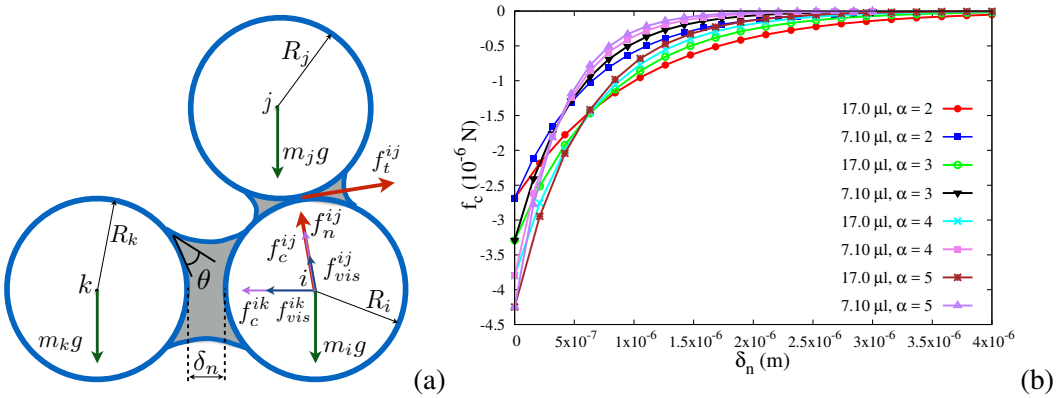

FIGURE 1 – (a) Schematic drawing of two different cases of capillary bridges : particle i in contact with particle j and without contact with particle k ; (b) Capillary cohesion force f_c as a function of the gap δ_n between two particles for different values of the liquid volume V_b (μl) and size ratio α.

The normal contact force f_n involves two components [13] :

$$f_n = f_n^e + f_n^d \,. \tag{2}$$

where $f_n^e = k_n\delta_n$ is the normal repulsive elastic force as a linear function of the normal elastic deflection δ_n (overlap between two particles), where k_n is the normal stiffness, and $f_n^d = \gamma_n\dot{\delta}_n$ is the normal damping force, proportional to the relative normal velocity $\dot{\delta}_n$, with γ_n as the normal viscous damping. These forces occur only when there is an overlap, i.e. for $\delta_n < 0$. The tangential contact force f_t is the sum of an elastic force $f_t^e = k_t\delta_t$ and a damping force $f_t^d = \gamma_t\dot{\delta}_t$, where k_t denotes the tangential stiffness, γ_t is the tangential viscous damping parameter, and δ_t and $\dot{\delta}_t$ are the tangential displacement and velocity, respectively. The tangential force is bounded by a force threshold μf_n according to the Coulomb friction law, where μ is the friction coefficient :

$$f_t = -\min\left\{(k_t\delta_t + \gamma_t\dot{\delta}_t), \mu f_n\right\}. \tag{3}$$

The capillary force f_c between two wet particles depends on the liquid volume V_b of the capillary bridge, liquid-vapor surface tension γ_s and particle-liquid-gas contact angle θ [14] ; see Fig. 1. The capillary force is determined by integrating the Laplace-Young equations. In the pendular state, an approximate solution is given by the expression [14, 12, 15] :

$$f_c = \begin{cases} -\kappa R, & \text{for } \delta_n < 0, \\ -\kappa R\, e^{-\delta_n/\lambda}, & \text{for } 0 \le \delta_n \le d_{rupt}, \\ 0, & \text{for } \delta_n > d_{rupt}, \end{cases} \tag{4}$$

where $R = \sqrt{R_i R_j}$ is the geometrical mean radius of two particles of radii R_i and R_j and the capillary force pre-factor κ is

$$\kappa = 2\pi\gamma_s\cos\theta. \tag{5}$$

This force exists up to a rupture distance d_{rupt} given by

$$d_{rupt} = \left(1 + \frac{\theta}{2}\right) V_b^{1/3} . \tag{6}$$

The characteristic length λ is the factor that denotes the exponential falloff of the capillary attraction force in equation (4) :

$$\lambda = c\, h(r) \left(\frac{V_b}{R'}\right)^{1/2} , \tag{7}$$

where $R' = 2R_iR_j/(R_i+R_j)$ and $r = \max\{R_i/R_j; R_j/R_i\}$ are the harmonic mean radius and the size ratio between two particles. The expression (4) nicely fits the capillary force as obtained from direct integration of the Laplace-Young equation by setting $h(r) = r^{-1/2}$ and $c \simeq 0.9$ [16].

The normal viscous force f_{vis} is due to the lubrication effect of liquid bonds between particles. Its expression for two spherical particles is [10, 15] :

$$f_{vis} = \frac{3}{2}\pi R^2 \eta \frac{v_n}{\delta_n}, \tag{8}$$

where η is the liquid viscosity and v_n denotes the relative normal velocity assumed to be positive when the gap δ_n is decreasing. This expression implies that the viscous force diverges when the gap δ_n tends to zero. We also introduce a characteristic length δ_{n0} representing the size of asperities and assume that the lubrication force is given by :

$$f_{vis} = \frac{3}{2}\pi R^2 \eta \frac{v_n}{\delta_n + \delta_{n0}} \quad \text{for } \delta_n > 0 . \tag{9}$$

In the case $\delta_n > 0$, i.e. for a positive gap, the singularity will not occur as long as there is no contact. When contact occurs, i.e. for $\delta_n < 0$, we assume that the viscous force depends only on the characteristic length :

$$f_{vis} = \frac{3}{2}\pi R^2 \eta \frac{v_n}{\delta_{n0}} \quad \text{for } \delta_n \leq 0 . \tag{10}$$

Here, we keep $\delta_{n0} = 5.10^{-4} d_{min}$. This value is small enough to allow the normal viscous forces to be effective without leading to its divergence at contact.

2.2 Granulation procedure

Figure 2(a) shows the 3D numerical model of a rotating drum defined as cylinder of length L and diameter d_c composed geometrically by the juxtaposition of polyhedral elements. This drum is closed by two end planes and it can rotate around y axis at a given rotation speed ω. In our simulations, the gravity is perpendicular to the rotation axis.

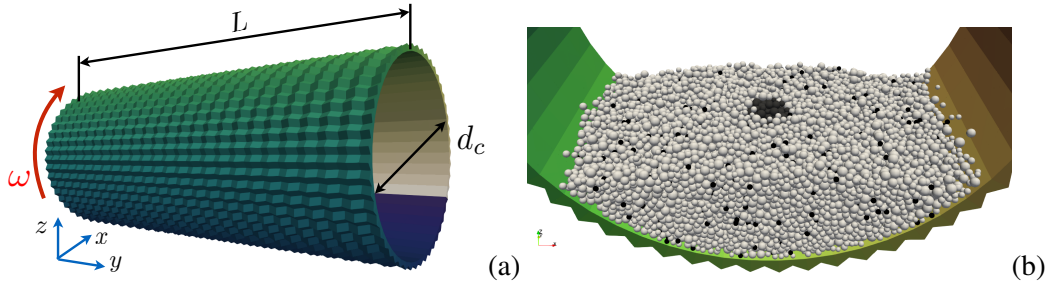

FIGURE 2 – (a) The geometry of the numerical drum, (b) initial distribution of dry (in gray) and wet (in black) particles with a single granule defined in the center top of the granular bed and 200 wet particles randomly distributed inside the bed.

The samples are composed of 5000 spherical particles placed inside a horizontal drum. All granular beds have the same filling level of $f = 20\%$ for different values of the size ratio. The size polydipersity of the particles is an important parameter defined by the ratio $\alpha = d_{max}/d_{min}$ between the largest and

TABLE 1 – Simulation parameters

Parameter	Symbol	Value	Unit
Minimum particle diameter	d_{min}	10	μm
Density of particles	ρ	3500	kg.m^{-3}
Size ratios	α	[1,5]	
Number of particles	N_p	5000	
Filling level	f	20	%
Friction coefficient	μ	0.5	
Normal stiffness	k_n	100	N/m
Tangential stiffness	k_t	80	N/m
Normal damping	γ_n	5.10^{-5}	Ns/m
Tangential damping	γ_t	5.10^{-5}	Ns/m
Surface tension	γ_s	0.072	N/m
Contact angle	θ	30.0	degree
Liquid viscosity	η	1.0	mPa.s
Time step	δt	10^{-7}	s

smallest particles. We considered three different size classes in a range $[d_{min}, d_{max}]$. Each size class has the same total volume so that the size distribution is uniform in terms of particle volumes. This distribution generally corresponds to a high packing fraction since small particles fill the pore space between large particles. In our simulations, the size of smallest particles d_{min} is considered to be constant whereas the size of largest particles d_{max} varies. All values of the system parameters used in the simulations are listed in Table 1

A single granule was defined by 100 wet particles inside a spherical probe located at the center top of the granular bed. 200 more wet particles were randomly distributed inside the drum. All other particles are considered to by dry. T he liquid content of wet particles is set to be $w = V_\ell/V_g = 0.09$, where V_ℓ denotes the liquid volume in the system and V_g is the wet particle volume. We also assume that there is no excess liquid so that a wet particle cannot form a liquid bridge with a dry particle. The granule size evolves by the accretion or erosion of wet particles. Fig. 2(b) shows the initial distribution of the granular bed together with the initial single granule and free wet particles randomly distributed when a steady flow state is reached by continuous rotation of the drum. As illustrated in Fig. 3, the wet particles represent actually micro-aggregates that are formed by the capillary action of small amounts of liquid. These micro-aggregates can transport the liquid during their motion and they can share their liquids upon collision to form larger aggregates.

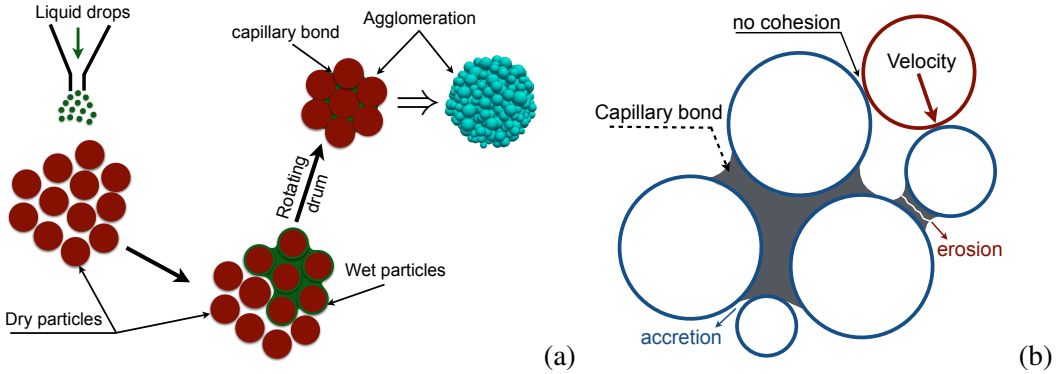

FIGURE 3 – (a) Schematic representation of the granulation model, (b) accretion and erosion phenomena of granule in the agglomeration process.

In order to study the effect of size ratio on the agglomeration process, we performed the granulation simulations by varying the values of the size ratio α in a range $[1,5]$. The flow regimes are controlled by the Froude number

$$Fr = \frac{\omega^2 d_c}{2g}, \tag{11}$$

Here, we set $Fr = 0.5$ in all simulations. This corresponds to a flow regime intermediate between the rolling regime and and cascading regime ($0.1 < Fr < 1$).

3 Granule growth

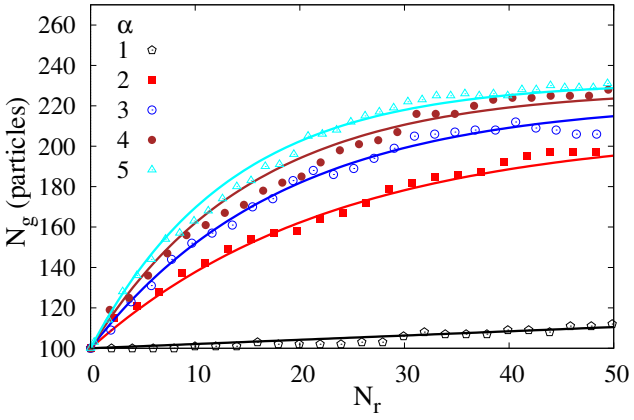

FIGURE 4 – Evolution of the granule size N_g (in number of particles) as a function of the number of drum rotations N_r for different values of size ratio α.

Figure 4 shows an almost exponentially increase of granule size, corresponding to the number N_g of wet particles inside agglomerate, as a function of the number N_r of drum rotations. Here, d_{min} is constant and equal to 10 μm. Hence, $d_{max} = \alpha d_{min}$ is variable depending on the size ratio α. The friction coefficient is set to $\mu = 0.5$. We observe that, except the mono-spheres case ($\alpha = 1$), for which the granule growth is a nearly linear function of the number of drum rotations, the total number of particles in single granule grows exponentially from the initial stage (100 wet spherical particles) to about its double after 50 drum rotations. The rate of the granule growth is proportional to the size ratio α and reaches the steady state after about 30 drum rotations. The exponential increase reflects the gradual decrease of the number of free micro-aggregates inside the granular bed.

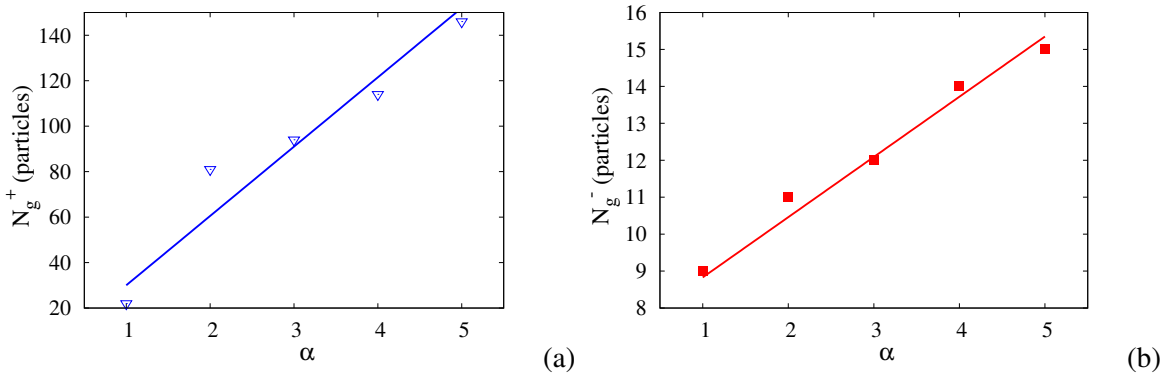

FIGURE 5 – Total number of the accreted particles N_g^+ and eroded particles N_g^- after 50 drum rotations as a function of the size ratio α.

The granule growth reflects the accretion and erosion phenomena during the granulation process. Figs. 5(a) and (b) show the total numbers of the accreted particles N_g^+ and the eroded particles N_g^- for different values of the size ratio α after 50 drum rotations. They increase quasi-linearly as a function of α. It can be explained by the increase of the normal and tangential forces between particles inside the granular flow as a result of the increase of α (or d_{max}) with a constant value of d_{min}.

4 Conclusions

In this paper, we investigated the granulation process of wet granular materials in a rotating drum by using a three-dimensional molecular dynamics simulations. The numerical method accounts for the cohesive and viscous effects of a small amount of a binding liquid added to the particles. We studied the growth of a single granule placed inside the granular bed. The granule size grows exponentially with the number of the drum rotations in the granular bed as a consequence of the gradual capture of wet particles by the initial single granule. The erosion rate increases as a linear function of the number of drum rotations whereas the cumulative number of accreted particles increases as an almost exponential function of the granulation time for the different values of polydispersity. The granule size growth slows down after several drum rotations as a result of the finite number of wet particles.

Acknowledgments

We gratefully acknowledge financial support by the Ministry of Education and Training in Vietnam and Campus France.

Références

[1] J. Litster and B. Ennis, *The Science and Engineering of Granulation Processes*, volume 15. Springer Netherlands, 2014.

[2] SM Iveson and JD Litster. *Growthregimemapforliquid-boundgranules*, AIChE, 44 (7) :1510-1518, 1998.

[3] B. J. Ennis, G. Tardos, and R. Pfeffer. *A microlevel-based characterization of granulation phenomena*, Powder Technology, 65(1) :257-272, 1991.

[4] F. Stepánek, P. Rajniak, C. Mancinelli, R.T. Chern, and R. Ramachandran. *Distribution and accessibility of binder in wet granules*, Powder Technology, 189(2) : 376-384, 2009.

[5] N. Rahmanian, A. Naji, and M. Ghadiri. *Effects of process parameters on granules properties produced in a high shear granulator*, Chemical Engineering Research and Design, 89(5) : 512-518, 2011.

[6] R.J. Spurling, J.F. Davidson, and D.M. Scott. *The transient response of granular flows in an inclined rotating cylinder*, Chemical Engineering Research and Design, 79(1) : 51-61, 2001.

[7] J.M.N.T. Gray. *Granular flow in partially filled slowly rotating drums*, Journal of Fluid Mechanics, 441 : 1-29, 2001.

[8] R. Ramachandran, JM.-H. Poon, CF.W. Sanders, T. Glaser, C. D. Immanuel, F J. Doyle, J D. Litster, F Stepanek, F-Y Wang, and I T. Cameron. *Experimental studies on distributions of granule size, binder content and porosity in batch drum granulation : Inferences on process modelling requirements and process sensitivities*, Powder Technology, 188(2) : 89-101, 2008.

[9] L. X. Liu, J. D. Litster, S. M. Iveson, and B. J. Ennis. *Coalescence of deformable granules in wet granulation processes*, AIChE Journal, 46 : 529-539, 2000.

[10] G. Lefebvre and P. Jop. *Erosion dynamics of a wet granular medium*, Physical Review E : Statistical, Nonlinear, and Soft Matter Physics, 8 : 032205, 2013.

[11] F. Radjai, V. Topin, V. Richefeu, C. Voivret, J-Y Delenne, E. Azéma, and M. S. El Youssoufi. *Force Transmission in Cohesive Granular Media*, Mathematical Modeling and Physical Instances of granular Flows, pages 240-260. AIP, 2010.

[12] T.-T. Vo, P. Mutabaruka, S. Nezamabadi, J-Y Delenne, E. Izard, R. Pellenq, and F. Radjai. *Mechanical strength of wet particle agglomerates*, Mechanics Research Communications, 92 : 1-7, 2018.

[13] T.-T. Vo, P. Mutabaruka, J.-Y. Delenne, S. Nezamabadi, and F. Radjai. *Strength of wet agglomerates of spherical particles : effects of friction and size distribution*, EPJ Web Conf., 140 : 08021, 2017.

[14] V. Richefeu, M.S. El Youssoufi, and F. Radjai. *Shear strength of unsaturated soils : Experiments, DEM simulations, and micromechanical analysis*, In Theoretical and Numerical Unsaturated Soil Mechanics, 83-91, 2007.

[15] T.-T. Vo, S. Nezamabadi, P. Mutabaruka, J.-Y. Delenne, E. Izard, R. Pellenq, and F. Radjai. *Particle dynamics simulation of wet granulation in a rotating drum*, Powder Technology, abs/1810.13438v1, 2019.

[16] F. Radjai and V. Richefeu. *Bond anisotropy and cohesion of wet granular materials*, Philosophical Transactions of the Royal Society A, 367 : 5123-5138, 2009.